Electrically tunable holographic polymer templated blue phase liquid crystal grating*

He Zheng-Hong(何正红)[a)b)], Chen Chao-Ping(陈超平)[a)†], Zhu Ji-Liang(朱吉亮)[a)], Yuan Ya-Chao(袁亚超)[a)], Li Yan(李 燕)[a)‡], Hu Wei(胡 伟)[a)], Li Xiao(李 潇)[a)], Li Hong-Jing(李洪婧)[a)], Lu Jian-Gang(陆建刚)[a)], and Su Yi-Kai(苏翼凯)[a)]

[a)] *National Engineering Laboratory for TFT-LCD Materials and Technologies, Department of Electronic Engineering, Shanghai Jiao Tong University, Shanghai* 200240, *China*

[b)] *School of Physical Science and Technology, Southwest University, Chongqing* 400715, *China*

(Received 14 September 2014; revised manuscript received 19 November 2014; published online 10 April 2015)

In this paper, we demonstrate an alternative approach to fabricating an electrically tunable holographic polymer templated blue phase liquid crystal grating. This grating is obtained by preforming a polymer template comprised of periodic fringes, and then refilling it with a blue phase liquid crystal. Compared with conventional holographic polymer dispersed liquid crystal gratings, our grating can remarkably reduce its switching voltage from 200 V to 43 V while maintaining a sub-millisecond response time. The holographic polymer templated blue phase liquid crystal (HPTBPLC) grating is free from electrode patterning, thus leading to a lower cost and more flexible applications.

Keywords: holographic polymer dispersed liquid crystal, blue phase, phase grating

PACS: 42.40.Eq, 61.30.Mp **DOI:** 10.1088/1674-1056/24/6/064203

1. Introduction

Holographic polymer dispersed liquid crystals (HPDLCs) have been extensively studied due to the high diffraction efficiency, fast response times, and easy fabrication.[1–5] They have potential applications in optical gratings, electro-optically addressable volume data storage, diffractive optical elements,[6–8] etc. Electrically switched distributed-feedback (DFB) lasing action was introduced with an HPDLC grating.[9,10] However, the switching electrical field of HPDLC is usually of the order of tens of volts per micrometer, which greatly hinders the practical applications of an HPDLC grating. This is primarily due to the large elastic deformation energy and the strong anchoring force associated with small liquid crystal droplet sizes.[11–13] For this reason, many researchers were dedicated to reducing the switching voltages of HPDLC devices.[11–14] Jang and Kim reported that the HPDLC is fabricated with the chemically incorporated graphene oxide, and the switching voltage is reduced from 70 V to 25 V; however, its decay time increases from 3.2 ms to 4.8 ms.[11] Sarkar *et al.* reported that the switching field decreases from 9 V/μm to 2.5 V/μm, by using partially fluorinated monomers, but the decay time increases from 1.6 ms to 18 ms.[12] Klosterman *et al*. reported that the switching field decreases from 12.5 V/μm to 5 V/μm, by adding the surfactant, but the decay time is longer.[14] In their work, the switching voltage was reduced, however, the decay time was longer.

Recently, the blue phase liquid crystal (BPLC) gratings based on patterned electrodes[15–17] and periodic polymer slices[18] have attracted substantial attention, because they exhibit high diffraction efficiency, fast response, etc. However, for BPLC gratings based on patterned electrodes, it is difficult to obtain high resolution because of the fringing electric field effect.[18] For BPLC gratings based on periodic polymer slices, the fabrication is relatively complicated.

In this paper, we demonstrate a holographic polymer templated blue phase liquid crystal (HPTBPLC) grating, which is obtained by replacing the nematic liquid crystal droplets with a BPLC composite in a conventional HPDLC grating. This HPTBPLC has a significantly reduced switching voltage (43 V) compared with the HPDLC grating (200 V), and the response time remains fast (< 1 ms). The fabrication of an HPTBPLC grating is free from electrode patterning, thus it could easily achieve high resolution and large diffraction angle at low cost.

2. Experiments

The fabrication process of making an HPTBPLC transmission grating is depicted in Fig. 1, where four stages are involved.

As shown in Fig. 1(a), at Stage 1, a uniform mixture fills

*Project supported by the National Basic Research Program of China (Grant No. 2013CB328804), the National Natural Science Foundation of China (Grant No. 61307028), the Funds from the Science and Technology Commission of Shanghai Municipality (Grant Nos. 11JC1405300, 13ZR1420000, and 14ZR1422300), and the Fundamental Research Funds for the Central Universities, China (Grant No. XDJK 2011C047).

†Corresponding author. E-mail: ccp@sjtu.edu.cn

‡Corresponding author. E-mail: yan.li@sjtu.edu.cn

© 2015 Chinese Physical Society and IOP Publishing Ltd

a cell via capillary action. The liquid crystal cell is formed by assembling two ITO glasses, with a gap held by spacers and the cell thickness d of 20 μm. In the experiments, the mixture comprises 21.9 wt%:7.5 wt%:1 wt%:0.6 wt%:69 wt% of TMPTA monomer (Aldrich): N-vinylpyrrollidone (Aldrich): N-phenylglycine (Aldrich): Rose Bengal (Aldrich): Nematic liquid crystal (BP-06, $\Delta n = 0.158$, $n_{\rm iso} = 1.56$, $\Delta\varepsilon = 34.2$, Jiangsu Hecheng Co.), and is made uniform by stirring in the dark.

As shown in Fig. 1(b), at Stage 2, the liquid crystal cell is first subjected to a holographic exposure to form an HPDLC grating. Two beams intersect inside the cell and produce an intensity distribution of the interference fringes. Two beams are derived from a diode solid-state laser (488 nm, 100 mW, Coherent) and set to be p-polarization. The intensity distribution at the cell can be expressed as $I(x) = I_0[1 + V\cos(\boldsymbol{K}\cdot\boldsymbol{x})]$, where $I_0 = 10.0$ mW/cm^2 is the total exposure intensity, V is a constant of fringe visibility and usually $V = 0.90$–0.95,[19] $\boldsymbol{K}$ is the grating vector with an amplitude $K = 2\pi/\Lambda$, and Λ is the grating period. The beam diameter D is 2.0 mm. A polymerization preferentially occurs in bright regions, creating a monomer concentration gradient between bright and dark regions, which causes the diffusions of monomers and liquid crystal molecules and then polymer-rich or polymer-poor regions appear.[19] An He–Ne laser ($\lambda = 632.8$ nm) beam, which is also set to be p-polarization with an incident angle being normal to the cell, is employed as the probe beam. The holographic grating is recorded for 20 s at an incident angle of 1.2° for each beam. Then, the cell is exposed to ultraviolet (UV) light to stabilize the HPDLC grating for 5 min.

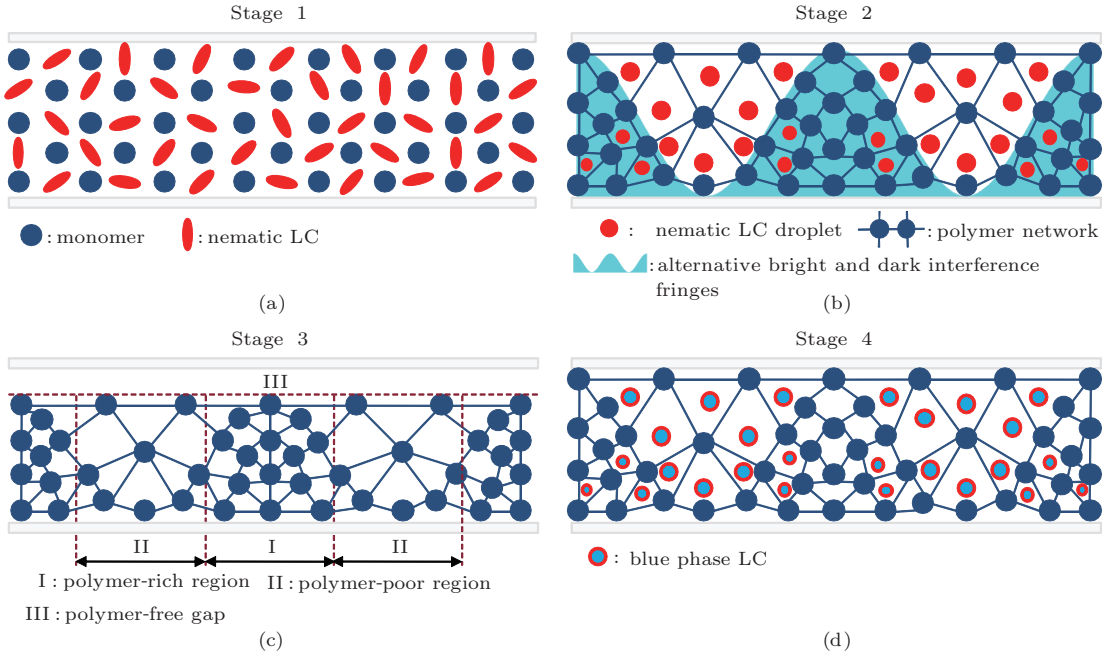


Fig. 1. (color online) Schematic diagrams of the fabrication procedure. (a) Stage 1: a mixture of monomers and liquid crystals fills the cell; (b) Stage 2: the HPDLC grating is formed under the alternating bright and dark interference fringes, then illuminated by an ultraviolet light to be stabilized; (c) Stage 3: the cell is immersed in acetone to wash out the liquid crystal and un-polymerized residuals. The remaining polymer template consists of the alternating polymer-rich and polymer-poor regions, which are denoted as regions I and II, respectively. A polymer-free gap is on the top of the polymer template, which is denoted as region III due to shrinking; and (d), Stage 4: the polymer template is refilled with a BPLC.

As shown in Fig. 1(c), at Stage 3, the polymer template is formed. The cell is immersed in acetone for 24 h. This could remove the liquid crystal droplets and non-polymerized residuals by diffusion.[20] When the cell is moved out of acetone, any acetone remaining in the cell evaporates quickly at room temperature. The remaining polymer template consists of the alternating polymer-rich and polymer-poor regions, which are denoted as regions I and II, respectively. After the polymerization, a polymer-free gap is formed on the top of the polymer template due to shrinking, which is denoted as region III. The scanning electron microscopy (SEM) images of the polymer template are shown in Figs. 2(a)–2(d). The grating period $\Lambda \approx 14$ μm, as shown in Figs. 2(a) and 2(b). The black and bright rectangle regions are located in the centers of polymer-poor and polymer-rich regions, respectively as shown in Fig. 2(a). The SEM images for black and bright rectangle regions are shown in Figs. 2(c) and 2(d), respectively. The statistical data for the black and bright rectangle regions are shown in Figs. 2(e) and 2(f), respectively. The average pore sizes in black and bright rectangle regions are 189.3 nm and 28.9 nm, respectively. The maximum sizes in the black and bright rectangle regions are 325 nm and 73 nm, and the minimum sizes in the black and bright rectangle regions are 83 nm and 13 nm, respectively, as shown in Figs. 2(e) and 2(f).

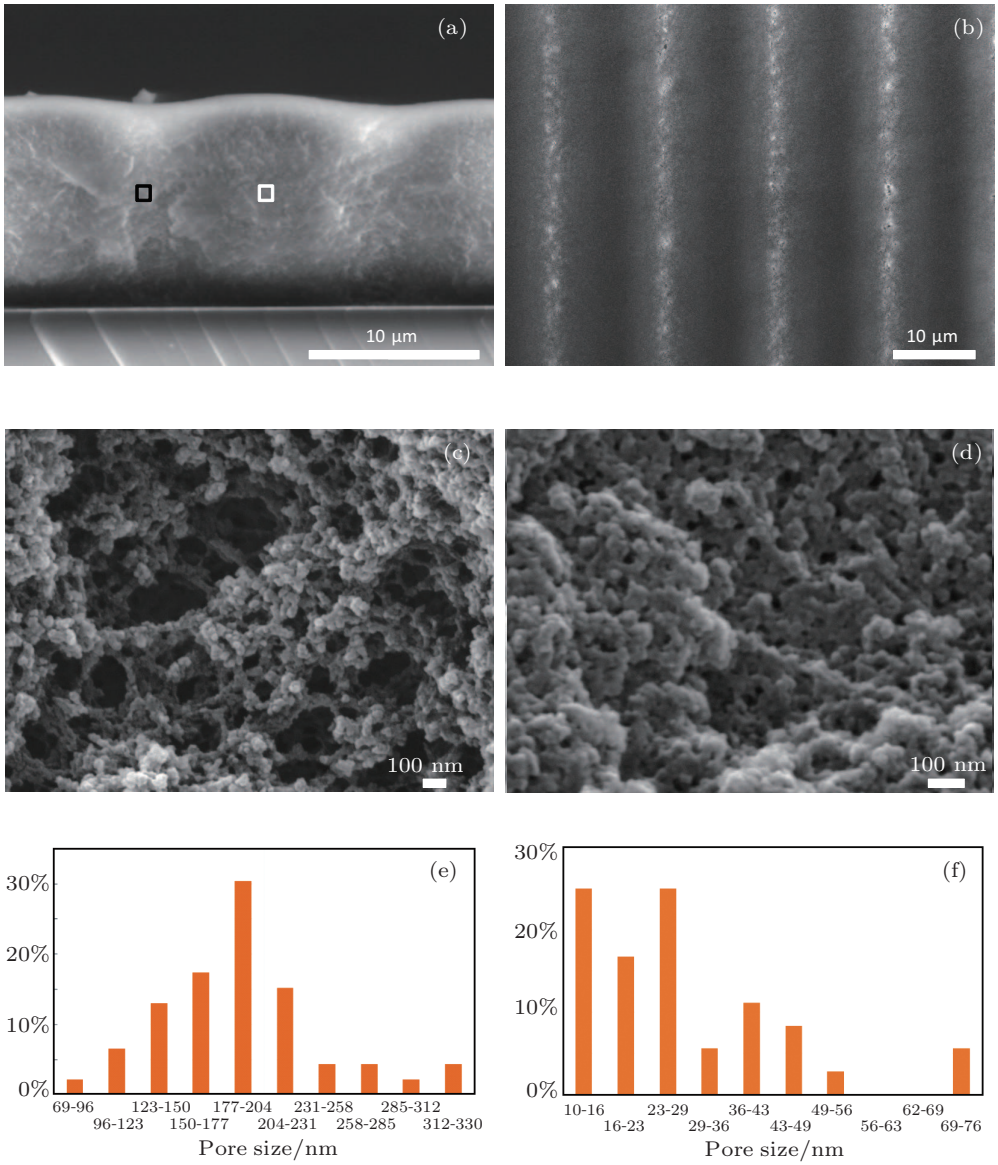


Fig. 2. (color online) SEM images and statistical data for the polymer template at Stage 3: (a) cross-sectional view of the polymer template, (b) top view of the polymer template, (c) cross-sectional view of the white rectangle region in the polymer-rich region, (d) cross-sectional view of the black rectangle in the polymer-poor region, (e) pore size distribution of the white rectangle region, and (f) pore size distribution of the black rectangle region.

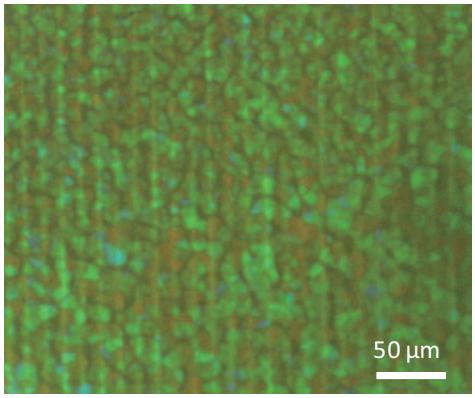


Fig. 3. (color online) Platelet textures observed with the optical polarizing microscope for the HPTBPLC grating at Stage 4 at 70.5 °C.

As shown in Fig. 1(d), at Stage 4, a BPLC fills the cell. The polymer template can undergo the reversible shrinking and swelling.[21–24] Because the polymer network is porous, a liquid crystal could be refilled into those voids, and region III could disappear due to re-swelling. The BPLC used is a mixture composed of the same nematic liquid crystal (96.5% BP-06, Jiangsu Hecheng Co.) for the HPDLC grating and the chiral dopant (3.5%, R5011, Jiangsu Hecheng Co.). Then the BPLC first fills the cell via capillary action at 80 °C, and then cooled down at a rate of 0.1 °C/min. The BPLC could form in polymer-poor region due to the relatively large pore sizes.[25] The temperature range for the BPLC in the HPTBPLC is from 69 °C to 72 °C. The morphology of the HPTBPLC grating is shown in Fig. 3, where the self-assembled BPLC shows a characteristic platelet texture based on the polymer template when it is observed in the reflective mode of an optical polarizing microscope. The different colors originate from different

orientations of cubic lattices.[26–31]

3. Results and discussion

Diffraction efficiencies versus applied voltages of HPDLC and HPTBPLC gratings are plotted in Fig. 4. The diffraction efficiency η is calculated as a ratio of the diffracted power of the first order to the total output power. For the HPDLC grating at Stage 2, $\eta = 15\%$ when the voltage is 0 V, the threshold voltage is 40 V and the switching voltage is 200 V at room temperature. For the HPTBPLC grating at Stage 4, no threshold voltage is observed, $\eta = 14.7\%$ when the voltage is 0 V and $\eta \approx 0\%$ at 43 V at 70.5 °C. The relatively low diffraction efficiency for the HPTBPLC comes from the small refractive index contrast. The refractive index of the polymer matrix is 1.527, and $n_{\rm iso} = 1.56$ for BP-06. If $n_{\rm iso}$ could be increased to 1.59, the maximum phase delay can reach π, and the first-order diffraction efficiency is 33%. Moreover, if the grating period is reduced or the cell thickness is increased, the HPTBPLC grating could become a volume grating possibly with a higher diffraction efficiency.[32–35]

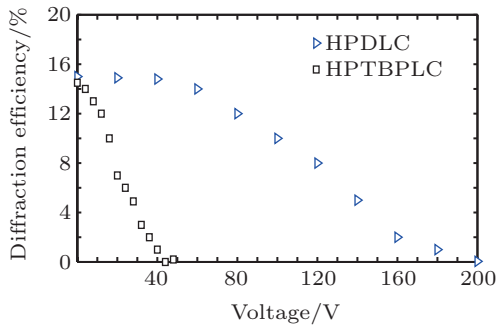


Fig. 4. (color online) Experimental results for the first-order diffraction efficiencies of HPDLC grating (triangles) and the HPTBPLC grating (squares), respectively.

The response times are also measured for the HPTBPLC and HPDLC gratings, and shown in Fig. 5. The cell is driven by a square-wave voltage with 1-kHz frequency. The dashed curve shows the first order transmittance of the HPDLC grating when it is switched between 0 V and 200 V. The solid curve shows the first order transmittance of the HPTBPLC grating switched between 0 V and 43 V. The rise and decay time are defined as 10% to 90% and 90% to 10% of the transmittance change, respectively. As shown in Fig. 5, the rise and decay time measured at room temperature are 341 μs and 424 μs for the HPDLC grating, respectively. While for the HPTBPLC grating, the rise and decay time measured at 70.5 °C are 610 μs and 890 μs, respectively.

The response times of both HPTBPLC and HPDLC are of the order of submillisecond but governed by different mechanisms. For HPDLC, typical response time varies from 25 μs to 1000 μs, depending on liquid crystal droplet size, elastic force strength, etc.[36,37] The HPTBPLC grating can maintain the fast response time because the BPLC can exhibit a fast response time.[26,27,31,39–41] Based on the Gerber model,[38] the decay time in a BPLC system can be expressed as

$$\tau = \frac{\gamma_1 P_{\rm DTC}^2}{k(2\pi)^2}, \tag{1}$$

where γ_1 denotes the rotational viscosity of a BPLC, k is the elastic constant, and $P_{\rm DTC}$ is the pitch length for a BPLC. From Eq. (1), the decay time is proportional to the square of the double twist cylinder pitch $P_{\rm DTC}$, which is determined by the concentration of chiral dopant.[39,40] Usually, if the concentration of chiral dopant is appropriate, a BPLC can exhibit a submillisecond graylevel (< 1 ms). In this work, with a 3.5%-concentration of chiral dopant R5011, the HPTBPLC has exhibited a slightly slower response than the HPDLC. The response time of the HPTBPLC could be further improved by increasing chiral dopant concentration (decreasing $P_{\rm DTC}$), but the tradeoff is the increased voltage.[39]

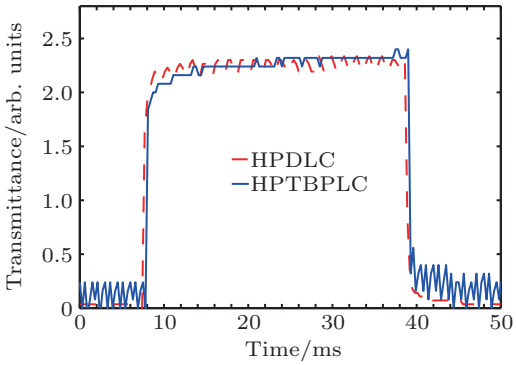


Fig. 5. (color online) Measured response times of the HPDLC (dashed curve) and HPTBPLC (solid curve) gratings.

The reduced switching voltage for the HPTBPLC is attributed to the weakened anchoring force and zero threshold voltage. First, the anchoring force is weakened in the HPTBPLC grating compared with that in the HPDLC grating. To verify the anchoring force change, another experiment is carried out by refilling the same liquid crystal at Stage 4 but without chiral dopant. The switching voltage is reduced from 201 V to 46 V, and the decay time is increased from 450 μs to several minutes due to the weakened anchoring force in polymer-poor regions after the wash-out process.[42] Second, there is no threshold voltage for the HPTBPLC. The HPTBPLC grating can be driven even with a very low operation voltage; however, for the HPDLC grating, the threshold voltage is 40 V as shown in Fig. 4. Moreover, the driving voltage for the BPLC without polymer stabilization is relatively low.[41,43] Therefore, the driving voltage for the HPTBPLC is reduced significantly.

The on-state transmittance of the HPTBPLC grating keeps increasing. The electro-optic response of a BPLC without polymer stabilization is fast with local director reorientation, but quite slow in the electrostriction region, at approximately dozens of milliseconds.[39] As a result, it takes a little longer time for some liquid crystals to restore to their original arrangement after the applied voltage has been removed. The transmittance fluctuation at off-state of HPTBPLC results from a poor dark state, because the electric field can affect the blue phase structure and stability.[44] As the electric field increases, it is possible for a BPLC that the local director reorientation, electrostriction, and field-induced phase transition are distinguished.[39,41,44]

The simulation work is performed to fit the experimental data. The BPLC consists of countless double-twist self-assembled liquid crystal cylinders stacked in three dimensions, forming a cubic symmetry. This structural symmetry induces the optical isotropy of a BPLC when the voltage is 0 V. The first-order diffraction efficiency can be expressed as[32]

$$\eta = \mathrm{J}_1^2\left(\frac{2\pi d\,(n_{\mathrm{I}}-n_{\mathrm{II}})}{\lambda}\right), \tag{2}$$

where J_1^2 is the first-order Bessel function of the first kind, d is the thickness of the grating, and n_{I} and n_{II} are the average refractive indices of the polymer-poor and polymer-rich regions, respectively, n_{I} and n_{II} are determined by the Lorentz–Lorenz relation:[45]

$$\begin{cases} \dfrac{n_{\mathrm{I}}^2-1}{n_{\mathrm{I}}^2+2} = \phi_{\mathrm{PI}}\dfrac{n_{\mathrm{p}}^2-1}{n_{\mathrm{P}}^2+2}+\phi_{\mathrm{LCI}}\dfrac{n_{\mathrm{lc}}^2-1}{n_{\mathrm{lc}}^2+2}, \\ \dfrac{n_{\mathrm{II}}^2-1}{n_{\mathrm{II}}^2+2} = \phi_{\mathrm{PII}}\dfrac{n_{\mathrm{p}}^2-1}{n_{\mathrm{P}}^2+2}+\phi_{\mathrm{LCII}}\dfrac{n_{\mathrm{lc}}^2-1}{n_{\mathrm{lc}}^2+2}, \end{cases} \tag{3}$$

where n_{p} is the refractive index of the polymer network, n_{lc} is the refractive index for the liquid crystal with an applied field, and the electric field is set to be perpendicular to the cell. Based on our previous work,[46] the average volume fractions of the polymer network in polymer-rich and polymer-poor regions can be estimated to be $\phi_{\mathrm{PI}} = 91\%$ and $\phi_{\mathrm{PII}} = 66\%$, respectively. The liquid crystal's volume fraction in the polymer-rich region, ϕ_{LCI}, equals $1-\phi_{\mathrm{PI}}$, and that in the polymer-poor region, ϕ_{LCII}, equals $1-\phi_{\mathrm{PII}}$. According to the experimental results (i.e., squares), when the applied voltage is 0 V, the diffraction efficiency is around 14.7%, arising from the refractive index contrast between polymer-rich and polymer-poor areas, and we obtain $n_{\mathrm{I}} = 1.530$ and $n_{\mathrm{II}} = 1.538$ from Eqs. (2) and (3). When the applied voltage increases, n_{II} decreases due to the decreased n_{lc} of the BPLC in polymer-poor regions. When the voltage reaches 43 V, n_{II} matches n_{I}, and the diffraction efficiency drops to zero.

4. Conclusions

In this paper, we demonstrate a holographic polymer templated blue phase liquid crystal grating. This device exhibits a significant improvement in lowering the switching voltage from 200 V to 43 V, while maintaining a sub-millisecond response time relative to an HPDLC grating. This promising approach could bring potential applications in optical switch, optical storage, electrically switchable lasers, etc.

References

[1] Yamane H, Kikuchi H and Kajiyama T 1999 *Polymer* **40** 4777
[2] Maschke U, Coqueret X and Benmouna M 2002 *Macromol. Rapid. Commun.* **23** 159
[3] Domash L, Crawford G, Ashmead A, Smith R, Popovich M and Storey J 2000 *SPIE* **4107** 46
[4] Sutherland R L, Natarajan L V, Tondiglia V P and Bunning T J 1993 *Chem. Mater.* **5** 1533
[5] Chen C P, Su Y and Jhun C G 2014 *J. Opt. Photon.* **1** 1
[6] Xiong Y, He Z H, Chen C P, Li X, Li A, Ye Z, Lu G, He G and Su Y 2013 *Opt. Commun.* **41** 296
[7] Sutherland R L, Tondiglia V P, Natarajan L V, Bunning T J and Adams W W 1994 *Appl. Phys. Lett.* **64** 1074
[8] Tondiglia V P, Natarajan L V, Sutherland R L, Bunning T J and Adams W W 1995 *Opt. Lett.* **20** 1325
[9] Hsiao V K S, Lu C, He G S, Pan M, Cartwright A N, Prasad P N, Jakubiak R, Vaia R A and Bunning T J 2005 *Opt. Express* **13** 3787
[10] Jakubiak R, Natarajan L V, Tondiglia V, He G S, Prasad P N, Bunning T J and Vaia R A 2004 *Appl. Phys. Lett.* **85** 6095
[11] Jang M W and Kim B K 2011 *J. Mater. Chem.* **21** 19226
[12] Sarkar M D, Qi J and Crawford G P 2002 *Polymer* **43** 7335
[13] Liu Y J, Sun X W, Dai H T, Liu J H and Xu K S 2005 *Opt. Mater.* **27** 1451
[14] Klosterman J, Natarajan L V, Tondiglia V P, Sutherland R L, White T J, Guymonc C A and Bunning T J 2004 *Polymer* **45** 7213
[15] Zhu J L, Lu J G, Qiang J, Zhong E W, Ye Z C, He Z H, Guo X J, Dong C Y, Su Y K and Shieh H P D 2012 *J. Appl. Phys.* **111** 033101
[16] Yan J, Li Y and Wu S T 2011 *Opt. Lett.* **36** 1404
[17] Zhu G, Li J N, Lin X W, Wang H F, Hu W, Zheng Z G, Cui H Q, Shen D and Lu Y Q 2012 *J. Soc. Inf. Display* **20** 341
[18] Yan J, Li Q and Hu K 2013 *J. Appl. Phys.* **114** 153104
[19] Qi J, Li L, De Sarkar M and Crawford G P 2004 *J. Appl. Phys.* **96** 2443
[20] Castles F, Day F V, Morris S M, Ko D H, Gardiner D J, Qasim M M, Nosheen S, Hands P J W, Choi S S, Friend R H and Coles H J 2012 *Nat. Mater.* **11** 599
[21] Urayama K 2007 *Macromolecules* **40** 2277
[22] McConney M E, White T J, Tondiglia V P, Natarajan L V, Yang D K and Bunning T J 2012 *Soft Matter* **8** 318
[23] Cazzell S A, McConney M E, Tondiglia V P, Natarajan L V, Bunning T J and White T J 2014 *J. Mater. Chem. C* **2** 132
[24] Urayama K, Okuno Y, Nakao T and Kohjiya S 2003 *J. Chem. Phys.* **118** 2903
[25] Jau H C, Lai W M, Chen C W, Lin Y T, Hsu H K, Chen C H, Wang C C and Lin T H 2013 *Opt. Mater. Express* **3** 1516
[26] Kikuchi H, Yokota M, Hiskado Y, Yang H and Kajiyama T 2012 *Nat. Mater.* **1** 64
[27] Yan J, Cheng H C, Gauza S, Li Y, Jiao M, Rao L and Wu S T 2010 *Appl. Phys. Lett.* **96** 071105
[28] Ge Z, Gauza S, Jiao M, Xianyu H and Wu S T 2009 *Appl. Phys. Lett.* **94** 101104
[29] Rao L, Ge Z, Wu S T and Lee S H 2009 *Appl. Phys. Lett.* **95** 231101
[30] Lin Y H, Chen H S, Lin H C, Tsou Y S, Hsu H K and Li W Y 2010 *Appl. Phys. Lett.* **96** 113505
[31] Coles H J and Pivnenko M N 2005 *Nature* **436** 997
[32] Liu Y J and Sun X W 2008 *Adv. OptoElectron.* **2008** 684349
[33] Wang X D, Wang X, He Y L, Zheng H B, Tan J C, Ding D Y and Zheng G W 2010 *Chin. Phys. B* **19** 074215

[34] Song J, Liu Y G, Xuan L, Zheng Z G, Zhang L L, Guo F Z, Li W C, Deng S P and Ma J 2008 *Chin. Phys. B* **17** 3227
[35] Colier R J, Burckhardt C B and Lin L Y 1973 *Optical Holography* (New York/London: Academic Press) p. 686
[36] Wu B G, Erdmann J H and Doane J W 1989 *Liq. Cryst.* **5** 1453
[37] Mormile P, Musto P, Petti L, Ragosta G and Villano P 2000 *Appl. Phys. B* **70** 249
[38] Gerber P R 1985 *Mol. Cryst. Liq. Cryst.* **116** 197
[39] Choi H, Higuchi H and Kikuchi H 2011 *Soft Matter* **7** 4252
[40] Chen Y, Yan J, Sun J, Wu S T, Liang X, Liu S H, Hsieh P J, Cheng K L and Shiu J W 2011 *Appl. Phys. Lett.* **99** 201105
[41] Chen K M, Gauza S, Xianyu H and Wu S T 2010 *J. Disp. Technol.* **6** 318
[42] Nie X, Lu R, Xianyu H, Wu T X and Wu S T 2007 *J. Appl. Phys.* **101** 103110
[43] Zhu J L, Ni S B, Zhong E W, Lu J G and Su Y K 2012 *SID Symposium Digest of Technical Papers* **43** 106
[44] Stegemeyer H, Blümel T, Hiltrop K, Onusseit H and Porsch F 1986 *Liq. Cryst.* **1** 3
[45] Aubrecht I, Miler M and Koudela I 1998 *J. Mod. Opt.* **45** 1465
[46] He Z H, Chen C P, Gao H Y, Shi Q, Liu S, Li X, Xiong Y, Lu J, He G and Su Y K 2014 *Liq. Cryst.* **41** 673